JACS Hosting Innovations

Contents List available at JACS Directory

Journal of Advanced Electrochemistry

journal homepage: http://www.jacsdirectory.com/jaec



A Novel Hybridization Indicator $Zn_2(ET)(pzdc)(\mu_3-OH)$ for the Electrochemical Determination of Breast Cancer Gene BRCA1

L. Liu¹, F. Sun¹, Y. Wang², C. Ding¹, H. Li^{1,*}

- ¹School of Chemistry and Environment, South China Normal University, Guangzhou, Guangdong 510006, P.R. China.
- ²Department of Pathology, Zhujiang Hospital, Southern Medical University, Guangzhou 510282, P.R China.

ARTICLE DETAILS

Article history: Received 16 March 2016 Accepted 29 March 2016 Available online 16 April 2016

Keywords: Electrochemical DNA Biosensor Zn₂(ET)(pzdc)(μ₃-OH) MWCNT-COOH Breast Cancer Gene

ABSTRACT

A novel and facile biosensor using Zn₂(ET)(pzdc)(μ_3 -OH) complex as hybridization indicator was developed and further applied to detect breast cancer DNA. The (Nb, Mn) codoped titanium oxide (TMN) and carboxylated multi-wall carbon nano-tube (MWCNT-COOH) was immobilized on the electrode surface to prepare the composite film modified electrode, fixed single-stranded DNA (ssDNA) on the modified electrode surface with EDC and NHS as activator. Then a novel and sensitive electrochemical DNA biosensor based on the TMN and MWCNT-COOH composite film was prepared. The properties of the modified electrode and the interaction between indicator and DNA were studied by scanning electron microscopy (SEM), fluorescence spectrum, UV-vis spectrum, cyclic voltammetry (CV) and electrochemical impedance spectroscopy (EIS). Under optimal conditions, the target single-stranded DNA (ssDNA) could be quantified ranging from 1×10^{-14} M to 1×10^{-6} M with good linearity (r=0.9991) and a low detection limit of 1.67×10^{-15} M(3σ , n=11). Results showed that the synergistic effect between TMN and MWCNT-COOH could improve the sensitivity of the biosensor, which has great potential application for fabrication of electrochemical biosensor.

1. Introduction

Breast cancer has become one of the most threatening diseases to women throughout the world [1]. BRCA1 is a tumor suppressor gene which when mutated is associated with the development of hereditary breast cancers. In sporadic tumors, although inherent gene mutations are rare, loss of BRCA1, resulting from reduced expression or incorrect subcellular localization is very important [2]. At present, some important detection methods such as DNA sequencing and single-strand conformation polymorphism analysis have been used for the early detection and characterization of the BRCA1 gene [3, 4]. However, these methods have some shortcomings such as low sensitivity, time consuming, high cost and so on. Therefore the development of a high sensitivity and high selectivity method for rapid detection of BRCA1 gene is of great scientific and practical importance. In recent years, DNA electrochemical sensor obtains a highly attention because of its simple preparation process, high sensitivity, good stability and good selectivity [5-8].

Carbon nanotube has been widely used in the field of electrochemical sensor for good biocompatibility, high mechanical strength, excellent magnetic property and wide electrochemical window [9, 10]. Recent years there are many semiconductor materials, such as TiO2 and ZnO, being employed for DNA electrochemical biosensor. (Nb, Mn)-codped TiO2 nanoparticles (TMN) which synthesized by ourselves were proved to possess high electrically active, large specific surface area and good biological molecular loading capacity, and it is expected to be used as a new electrical activity marker and biomolecule immobilization platform. The two nanomaterials combined to form a nanocomposite material which can produce some unique properties.

Metal complexes are of great value in the field of the design of new anticancer drugs, molecular biology, DNA molecular switch. So the interaction theory and mode of metal complex with DNA have also become a hot topic in the research of biological science [11-15].

In this study, a new type of DNA electrochemical biosensor was prepared by $Zn_2(ET)(pzdc)(\mu_3$ -OH) metal complex as hybridization indicator, synthetic TMN and carboxylated multi-wall carbon nanotube

composite as electrode materials, EDC and NHS as an activator to make ssDNA molecules immobilize on the TMN/MWCNT-COOH/ITO modified electrode surface.

2. Experimental Methods

2.1 Reagents and Materials

 $Zn_2(ET)(pzdc)(\mu_3\text{-}OH)$ was provided by the author of the reference [16]. N, N-dimethyl Formamide (DMF) was purchased from Tianjin Baishi chemical industry Co., Ltd (Tianjin, China). Multi-walled carbon nanotubes (MWCNTs) was purchased from Shenzhen Nanotech Port Co., Ltd. N-hydroxy succinimide (NHS), 1-ethyl-3-(3-dimethyl aminopropyl) carbodiimide (EDC) and Chitosan (M.W. 100000 - 300000, deacetylation degree $\geq 85\%$), dilute nitric acid and other chemicals were obtained from Aladdin Reagent Company (Shanghai, China). All chemicals were of analytical reagent grade. The sterilized and deionized water was used in all solutions.

Indium-tin-oxide (ITO) coated glass plates have been obtained from Zhuhai Kaiva Electronic Components Co., Ltd.

The 26-base oligonucleotides probe (S1), target complementary sequence DNA (S2), one-base mismatched ssDNA (S3), two-base mismatched ssDNA (S4) and non-complementary sequence DNA (S5) were synthesized by Shanghai Invitrogen Co., Ltd. (China), which were related to the gene sequence of breast cancer. Their base sequences were as below Table 1.

Table 1 Oligonucletide sequences used in this study

Oligonucletide	Sequnce
Probe DNA (S1)	5'-ATGTATGAATTATAATCAAAGAAACC-3'
$(Mr = 8.586 \times 10^3 \text{ ug/umole})$	
Target DNA(S2)	5'-GGTTTCTTAGATTATAATTCATACAT-3'
$(Mr = 8.301 \times 10^3 \text{ ug/umole})$	
One-base-mismatch(S3)	5'-GGTTTCTTTGATTATGATTCATACAT-3'
$(Mr = 8.746 \times 10^3 \text{ ug/umole})$	
Two-base-mismatch(S4)	5'-GGTTGCTTTGATTATGATTCATACATG-3'
$(Mr = 8.621 \times 10^3 \text{ ug/umole})$	
Non-complementary(S5)	5'-CTTCTGGTAGTCGGAGCTGATGGCG-3'
$(Mr = 8.705 \times 10^3 \text{ ug/umole})$	

All DNA stock solutions (100 mg/L) were prepared with TE solution (10 mM Tris–HCl, 1 mM EDTA, pH 8.00) and stored at 4 $^{\circ}$ C.

^{*}Corresponding Author Email Address: analchemlh@163.com (He Li)

2.2 Apparatus

Electrochemical measurements were recorded using an Autolab Potentiostat/Galvanostat (Metrohm). A conventional three-electrode cell with an Ag/AgCl reference a platinum wire counter and the modified ITO as the working electrodes were used. Scanning electron micrograph (SEM) was obtained on Zeiss Ultra55 field emission scanning electron microscope (Carl Zeiss, Germany). Fluorescence intensity was measured using a Hitachi F-2500 fluorescence spectrophotometer.

2.3 Synthesis of TMN Nanostructures

The TMN nanostructures were synthesized by Sol-Gel method. 1 mL citric acid was dissolved in 100 mL deionized water at 80 °C, then 5 mL nitric acid and 0.5 mL tetrabutyl titanate were added and stirred for 2 h until it was clear then added ammonia to control its PH between 7 and 8. Subsequently, 1 mL niobium acid ammonium oxalate hydrates and 1 mL manganese nitrate were added into the solution with constant stirring for 2 h to gain uniform solution then the mixture was put in oven at 250 °C for 2 h to obtain inflating and obtained flocculent material. Eventually, the assynthesized precursors were calcined in muffle furnace for 6 h to obtain TMN nanostructures.

2.4 Spectrum Study

The optimal excitation wavelength of $Zn_2(ET)(pzdc)(\mu_3$ -OH) in fluorescence spectrum study is 280 nm and emission wavelength is 563 nm. Under the condition of excitation and emission slit width were both 5 nm. To investigate UV-vis spectrum, $5.00\times 10^{-5}~\text{molL}^{-1}~Zn_2(ET)(pzdc)(\mu_3$ -OH) solution, $1.00\times 10^{-6}~\text{molL}^{-1}~\text{dsDNA}$ and TE buffer solution were added into a 10 mL volumetric flask, then placed it at room temperature for specified time. After the reaction reached equilibrium the solution was scanned from 280 nm to 450 nm.

2.5 Electrochemical Study

Electrochemical measurements were investigated by cyclic voltammetry (CV), differential pulse voltammetry (DPV) and electrochemical impedance spectroscopy (EIS). 10 μ L of Zn₂(ET)(pzdc)(μ ₃-OH) solution was dropped on the ssDNA and dsDNA modified electrode, respectively. After drying, they were measured in 0.01 M PBS (pH 7.0) containing 5 mM [Fe(CN)₆]^{3-/4-} solution and 0.1 M KCl.

2.6 Fabrication of the DNA Electrochemical Biosensor

Before modification, cleaned the ITO electrode with acetone, ethanol, and deionized water, respectively, and then dried in air at room temperature.

(Nb, Mn)-codped TiO $_2$ nanoparticles (TMN) were synthesized by sol-gel method. The commercially available MWNTs functionalized with carboxylic acid groups were prepared by sonicating the MWCNTs in concentrated HNO $_3$ -H $_2$ SO $_4$ (V/V, 3:1) for 6 h, then washed repeatedly with deionized water till neutral and dried under vacuum condition.

A certain amount of MWCNT-COOH was suspended in 5 mL DMF under sonication, then the synthetic TMN powder was added to the suspension, ultrasonic dispersion 6 h at room temperature to obtained high dispersion suspension. 10 μL of the above solution was dropped onto the surface of the ITO electrode and dried in air at room temperature to form a layer of dry and stable composite membrane, then rinsed with deionized water and dried to get a modified electrode denoted as TMN/MWCNT-COOH/ITO. The modified electrode was immersed into PBS buffer (pH 7) containing EDC and NHS for 1h to active the carboxyl group, then it was washed with PBS buffer and deionized water, dried in air at room temperature and subsequently 10 μL of 1.0 \times 10-6 molL-1 ssDNA (S1) was dropped onto the surface of the activated electrode and dried in air at room temperature.

2.7 DNA Hybridization and Indicator Intercalating

The hybridization reaction was carried out by dropping 10 μ L of 1.0 × 10⁻⁶ molL⁻¹ complementary (S2), 1-base mismatched (S3), 2-base mismatched (S4), and non-complementary (S5) target DNA sequences onto the activated electrode, respectively. And then the electrode was rinsed with TE buffer and deionized water to remove the unhybrided DNA after keeping at 45 °C for 30 min. The hybridized electrodes are as follows: S2-S1/TMN/MWCNT-COOH/ITO, S4-S1/TMN/MWCNT-COOH/ITO and S5-S1/TMN/MWCNT-COOH/ITO.

The S2-S1/TMN/MWCNT-COOH/ITO electrode was immersed in $5.0 \times 10^{-3} \text{ molL}^{-1} \text{ Zn}_2(\text{ET})(\text{pzdc})(\mu_3\text{-OH})$ solution for 10 min at room temperature and then rinsed with TE buffer and deionized water to remove extra Zn₂(ET)(pzdc)(μ_3 -OH).

A schematic illustration of the fabrication and detection process of the DNA biosensor was shown in Fig. 1.

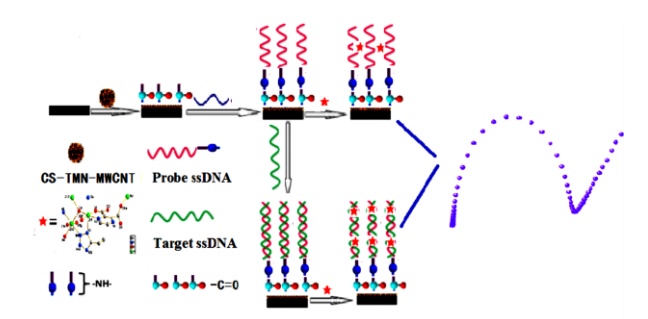
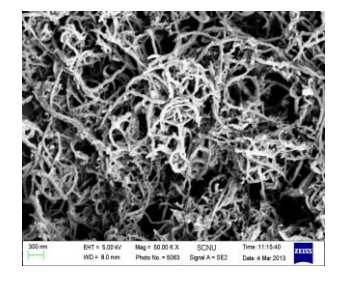


Fig. 1 Scheme of the DNA electrochemical biosensor

3. Results and Discussion

3.1 Scanning Electron Microscopy Studies

The scanning electron microcopy was employed to characterize the surface morphology changes of the electrode after hybridization. Fig. 2(A) showed the surface morphology of the ssDNA/TMN-MWCNT-COOH/ITO electrode. As can be seen from the figure the fusiform smooth and porous composite membrane was covered by the DNA probe and its structure was arranged orderly and uniform. It indicated that the DNA probe was successively immobilized on the electrode surface. Fig. 2(B) showed the surface morphology of the dsDNA/TMN-MWCNT-COOH/ITO electrode. It can be seen from the figure the modified electrodes appeared translucent after the dsDNA molecule assembly and its surface brightness increased significantly. It was mainly caused by dsDNA molecules which is nonconductive. So we can infer that DNA probe was hybridized with its complementary target DNA.



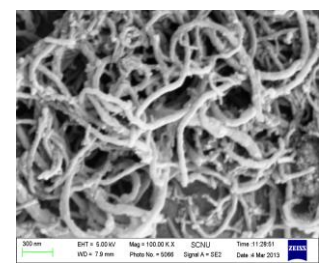


Fig. 2 SEM of (A) ssDNA/TMN-MWCNT-COOH/ITO electrode and (B)dsDNA/TMN-MWCNT-COOH/ITO

3.2 Fluorescence Spectrum

The difference of $Zn_2(ET)(pzdc)(\mu_3-OH)$ metal complex combined with ssDNA and dsDNA was investigated. $Zn_2(ET)(pzdc)(\mu_3-OH)$ was respectively added into ssDNA and dsDNA solution and then the blend system was studied by fluorescence spectrum. The results shown in the Fig. 3 below when the metal complex was added into the ssDNA solution, there was a weak fluorescence signal. But added into dsDNA solution the fluorescence intensity increased significantly. It was mainly because the protective effect of hydrophobic double-helix DNA molecules can enhance the fluorescent intensity of the metal complex [17]. Thus, we come to the conclusion that $Zn_2(ET)(pzdc)(\mu_3-OH)$ had combined with the double-helix structure of dsDNA.

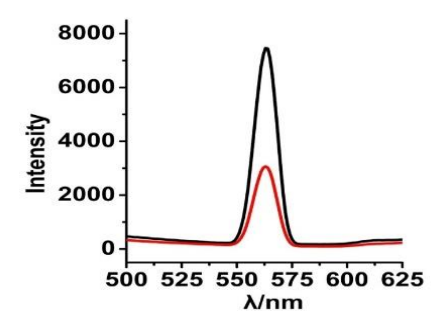


Fig. 3 The effect of $\rm Zn_2(ET)(pzdc)(\mu_3\text{-}OH)$ on the fluorescence spectra of ssDNA and dsDNA

3.3 UV-Vis Spectrum

The UV-vis absorption spectroscopy of the interaction between Zn(II) complex and DNA was shown in Fig. 4. As can be seen that the $Zn_2(ET)(pzdc)(\mu_3-OH)$ solution had a absorption peak at 300 nm. When the DNA was added, the hypochromic effect appeared. It was mainly because the ligand of the metal complex was intercalated into duplex DNA, and caused the empty π -orbital of the ligand appeared couple effect with the π -orbital of the DNA base pair. Meanwhile, the coupled π -orbital was partly filled with electronic and then the probability of π - π * transition reduced which caused hypochromic effect [18, 19]. The interaction of DNA molecules with small molecules will cause blue shift (red shift) or hypochromic (hyperchromic) effect. The formation of iso-absorptive point the red shift of absorption band and the decrease of absorbance can all illustrate that the small molecules was intercalated into duplex DNA. But there was no red shift phenomenon which indicates that the energy of π - π^* transition had not decreased. The result provided further evidence that the interaction between Zn₂(ET)(pzdc)(µ₃-OH) and DNA was weak.

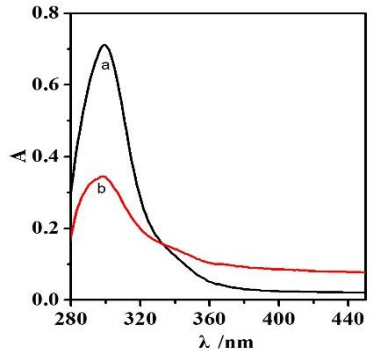


Fig. 4 The UV-vis spectrum of (a) $Zn_2(ET)(pzdc)(\mu_3-OH)$, (b) $Zn_2(ET)(pzdc)(\mu_3-OH)$ + DNA

3.4 Electrochemical Study

The interaction of $Zn_2(ET)(pzdc)(\mu_3-OH)$ and DNA was investigated by using electrochemical method. Fig. 5 showed the cyclic voltammograms of (a) the metal complex and (b) the metal complex after interacting with DNA for 10 min. It can be seen that both the oxidation peak and the reduction peak currents decreased and the peak potentials also shifted positively after adding DNA. It indicated that the metal complex was combined with DNA effectively. According to the theory of proposed by Bard [20], we can further prove that $Zn_2(ET)(pzdc)(\mu_3-OH)$ was intercalated into the base pairs of DNA.

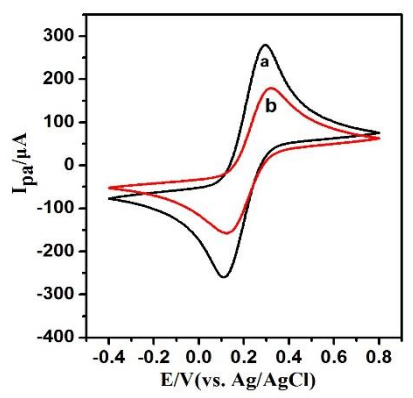


Fig. 5 Cyclic voltammograms of $Zn_2(ET)(pzdc)(\mu_3\mbox{-}OH)$ in the absence and presence of DNA

3.5 Effect of pH on the Interaction Between $Zn_2(ET)(pzdc)(\mu_3-OH)$ and DNA

The effect of pH on the interaction between the metal complexes with DNA was also studied. The changes of oxidation peak current differential (Δ Ipa) of modified electrode after interacting in PBS buffer solution of different pH value The change of oxidation peak current of dsDNA modified electrode after interacting with Zn₂(ET)(pzdc)(µ₃-OH) in the PBS buffer solution with different pH value was shown in Fig. 6. It can be seen from the graph the changes of peak current differential increased with increasing pH from 4.5 to 6.5 and decreased with the variation of pH from 6.5 to 8.5. The peak current differential is the largest when pH is 6.5, which indicates that the interaction between DNA and Zn₂(ET)(pzdc)(µ₃-OH) is the strongest. It was caused by that too high acidity will damage the structure of the dsDNA molecule, and too low acidity might enhance the

repulsion between the metal complex and negatively charged phosphate backbone of DNA molecular. So the optimal pH 6.5 of the working buffer was chosen in the further studies.

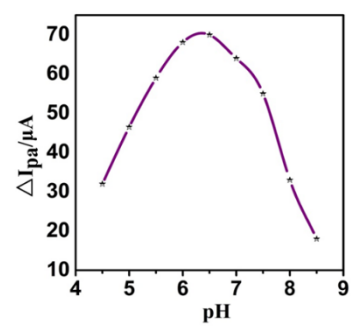


Fig. 6 The relationship of ΔI_{pa} and pH

3.6 Effect of Time on the Interaction between $Zn_2(ET)(pzdc)(\mu_3-OH)$ and DNA

Interaction Time of 2, 4, 6, 8, 10, 12 and 14 min were selected to test the sensitivity of the sensor. And the electrochemical signals of the electrodes were measured. It can be seen from the Fig. 7, the oxidation peak current decreased with the increment of interaction time and when the interaction time was more than 10 min, it tended to be stable, indicating that the interaction between DNA with $Zn_2(ET)(pzdc)(\mu_3-OH)$ metal complex had reached saturated. Therefore, the optimal interaction time between DNA with $Zn_2(ET)(pzdc)(\mu_3-OH)$ complex was chosen to be 10 min.

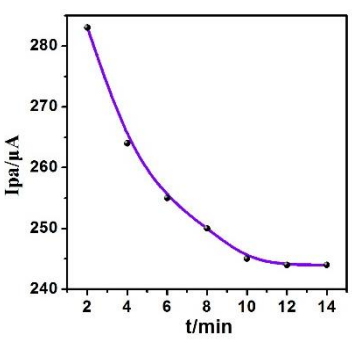


Fig. 7 The relationship of I_{pa} and the interaction time

3.7 Effect of DNA Concentration on the Oxidation Peak Current of $Zn_2(ET)(pzdc)(\mu_3$ -OH)

The oxidation peak currents of different concentrations of DNA interacted with $\rm Zn_2(ET)(pzdc)(\mu_3\text{-}OH)$ were shown in Fig. 8. It can be seen that the oxidation peak current of the modified electrodes decreased with the increment of the concentration of DNA. When the concentration increases to 1.5 \times 10^{-6} molL-1, concentrations reached saturation and current signal had not changed showing that the oxidation peak current of the modified electrodes reached a plateau.

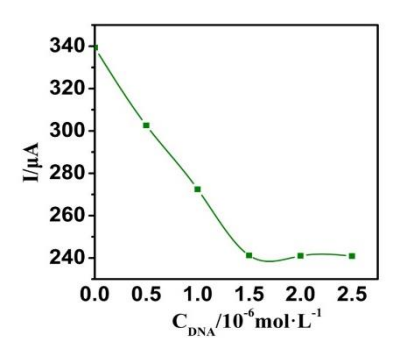


Fig. 8 The relationship between Ipa and $C_{\mbox{\scriptsize DNA}}$

3.8 Electrochemical Characterization of Modified Electrode

The CV response of modified electrodes in PBS buffer solution(pH = 7) including 5 mM [Fe(CN) $_6$]^{3-/4-} solution and 0.1 M KCl was shown in the Fig. 9. It was obvious that the peak current of TMN/MWCNT-COOH/ITO electrode (curve d) was higher than that of the MWCNT-COOH/ITO electrode (curve c) and TMN/ITO electrode (curve b). It indicated that there was an obvious synergistic effect of TMN and MWCNT on enhancement of the conductivity of electrode. Meanwhile TMN

nanomaterials could effectively increase the electrochemically active specific surface area, and provide a highly efficient platform for immobilizing biomolecules.

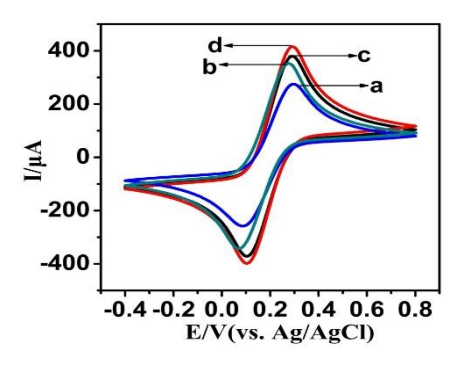


Fig. 9 CV of (a) ITO, (b) TMN/ITO, (c) MWCNT-COOH/ITO and (d) TMN/MWCNT-COOH/ITO in PBS buffer solution (pH = 7) including 5 mM [Fe(CN) $_6$]^{3-/4-} solution and 0.1 M KCl.

Fig. 10 showed the Nyquist diagrams of different modified electrodes in PBS buffer solution (pH = 7) including 5 mM [Fe(CN)6]3–/4– solution and 0.1 M KCl. At the bare ITO (curve a), the electron-transfer resistance (Ret) which corresponds to the semicircle diameter can be estimated to be 503 Ω . The Ret of TMN/ITO and MWCNT-COOH/ITO electrodes (curves b and c) decreased dramatically which was due to the high electrical conductivity of TMN and MWCNT. At TMN/MWCNT-COOH/ITO electrode, the Ret value decreased to 99 Ω (curve d), reduced obviously comparing to that of TMN/ITO and MWCNT-COOH/ITO electrodes (curves b and c). It attributed to the strong interaction between functionalized MWCNT and TMN, which enhanced specific surface area and electrical conductivity of the composite membrane.

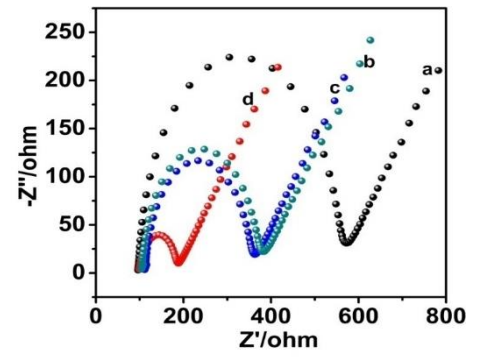


Fig. 10 EIS of (a) ITO, (b) TMN/ITO, (c) MWCNT-COOH/ITO and (d) TMN/MWCNT-COOH/ITO in PBS buffer solution (pH = 7) including 5 mM [Fe(CN)₆]^{3-/4-} solution and 0.1 M KCl

3.9 Selectively of the Novel DNA Electrochemical Biosensor

With $Zn_2(ET)(pzdc)(\mu_3-OH)$ as hybridization indicator, the selectivity of a novel DNA electrochemical biosensor was studied by employing differential pulse method. In this study, functionalized DNA probe was hybridized with four different types of target DNA including complementary, single-base mismatch, double-base mismatch and noncomplementary sequences. The results are shown in Fig. 11. The change of the peak current of DNA hybridization with complementary sequence was largest (b), while the DNA probe was hybridized with single-base mismatch sequences (e) and double-base mismatch sequences (d), the electrochemical signals reduced in turn. When the DNA probe hybridized with non-complementary sequence(c), the peak current response was the same as the DNA probe, indicating that there was no hybridization reaction to form the DNA double helix structure.

3.10 Electrochemical Impedance Spectrum (EIS)

Under the optimal experimental conditions, the proposed ssDNA/TMN/MWCNT-COOH/ITO electrode was used to hybridize with the different concentration of target DNA and the Nyquist diagrams of dsDNA/TMN/MWCNT-COOH/ITO electrode was measured in PBS buffer solution (pH = 7) including 5 mM [Fe(CN)₆]^{3-/4-} solution and 0.1 M KCl. Fig. 12 showed that with increasing of DNA probe concentration, the diameter of EIS increased, indicating that the electron transfer between electrode surface and solution became more and more difficult. According to the Nyquist diagrams, the average value of Δ Ret was proportional to the

logarithm of DNA probe concentration in the range from 1.0×10^{-14} M to 1.0×10^{-6} M with a regression equation. The linear regression equation was as follows:

$$\Delta R_{et} = 48.98 \lg(C/M) + 843.46 R^2 = 0.9991$$
 (1)

Where, $\triangle R_{et}$ was the change of peak current response, ($\triangle R_{et} = R_{before} - R_{after}$), before and after the probe DNA reaction with the target DNA C was the concentration of target DNA R^2 was the relative standard deviation.

A detection limit of the breast cancer gene sequence was determined to be 1.67 \times $10^{-15}\,M$ (3 σ) (where σ is the relative standard deviation of the blank solution, n = 11), suggesting that the proposed DNA biosensor is good enough for the breast cancer gene sequence detection.

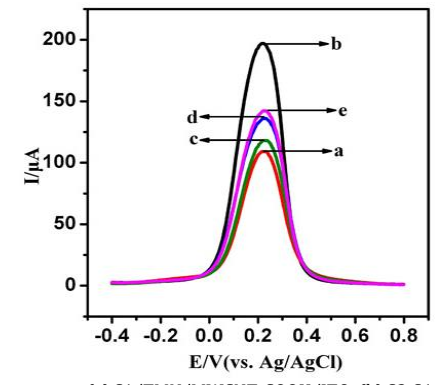


Fig. 11 DPV response at (a) S1/TMN/MWCNT-COOH/ITO; (b) S2-S1/TMN/MWCNT-COOH/ITO; (c) S5-S1/TMN/MWCNT-COOH/ITO; (d) S4-S1/TMN/MWCNT-COOH/ITO and (e) S3-S1/TMN/MWCNT-COOH/ITO in PBS buffer solution (pH = 7) including 5 mM [Fe(CN) $_6$]3-/4- solution and 0.1 M KCl

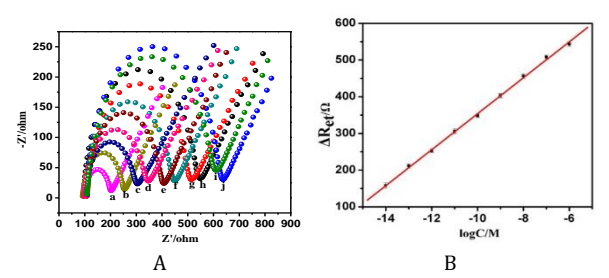


Fig. 12 (A) Nyquist diagrams of ssDNA/TMN/MWCNT-C00H/ITO(a) and DNA hybridization with its complementary target DNA under various concentrations: (b) $1.0 \times 10^{-14} \, \text{M}$; (c) $1.0 \times 10^{-13} \, \text{M}$; (d) $1.0 \times 10^{-12} \, \text{M}$; (e) $1.0 \times 10^{-11} \, \text{M}$; (f) $1.0 \times 10^{-10} \, \text{M}$; (g) $1.0 \times 10^{-9} \, \text{M}$; (h) $1.0 \times 10^{-8} \, \text{M}$; (i) $1.0 \times 10^{-7} \, \text{M}$ and (j) $1.0 \times 10^{-6} \, \text{M}$; (B) The calibration plot of Ret against the logarithm of the BRCA1 gene segment concentration

3.11 Reproducibility and Regeneration of the DNA Biosensor

In this study, ssDNA/TMN/MWCNT-COOH/ITO electrode was immersed into hot water at 80 °C for 20 min, then placed in the refrigerator at 4 °C to cool for 20 min, repeat five times. The DPV response of the electrode reduced about 17% compared with its original signal. This was possibly because the ssDNA probe which covalently immobilized on the electrode surface might fall off when the sudden change in temperature. At the same time, the stability of the DNA electrochemical biosensor was investigated. The dsDNA/TMN/MWCNT-COOH/ITO electrode was stored in the refrigerator at 4 °C for 15 days. And the DPV response reduced 8% compared with its initial current after 15 days of storage. The results showed that the novel DNA biosensor based on TMN/MWCNT-COOH nanocomposites possessed good regenerative capacity and stability.

4. Conclusion

In this paper, $Zn_2(ET)(pzdc)(\mu_3-OH)$ metal complex as a hybridization indicator was first introduced and applied to the detection of breast cancer gene. The experimental results showed that the metal complex was mainly combined with double stranded DNA molecule by intercalating effect. And the novel electrochemical biosensor used the synergistic effect between TMN and MWCNT-COOH to improve the sensitivity of the sensor. The proposed DNA biosensor has the feature of a wide linear range, low detection limit, high sensitivity, good stability and selectivity. In summary, bioelectrode based $Zn_2(ET)(pzdc)(\mu_3-OH)$ as a novel hybridization indicator provides an excellent sensing platform for efficient detection of DNA.

Acknowledgements

This work was supported by the Science and Technology Planning Project of Guangzhou (No. 2009Z2-D511), the Natural Science Foundation Guangdong Province (Nos. 101510631-01000011 S2011040003162), and Guangzhou Key Laboratory of Analytical Chemistry for Biomedicine (No. 201509010001), China.

References

- S. Zhu, Y. Cao, Z. Ye, Y. Yin, X. Zhu, Electrochemical assay of the relationship between the inhibition of phosphatidylinositol 3-kinase pathway and estrogen receptor expression in breast cancer, Anal. Bioanal. Chem. 405 (2013) 9593-
- E.A. Rakha, S.E. El-Sheikh, M.A. Kandil, M.E. El-Sayed, A.R. Green, Ian O.Ellis, Expression of BRCA1 protein in breast cancer and its prognostic significance, Human Pathol. 39 (2008) 857-865.
- P. Abdul Rasheed, N. Sandhyarani, Attomolar detection of BRCA1 gene based on gold nanoparticle assisted signal amplification, Biosens. Bioelectron. 65(3) (2015) 33-340.
- J. Nie, D.W. Zhang, T. Cai, Y.L. Zhou, X.X. Zhang, A label-free DNA hairpin biosensor for colorimetric detection of target with suitable functional DNA partners, Biosens. Bioelectron. 49 (2013) 236-242.
- J. Wang, X. Cai, G. Rivas, H. Shiraishi, P.A. Farias, N. Dontha, DNA electrochemical [5] biosensor for the detection of short DNA sequences related to the human immunodeficiency virus, Anal. Chem. 68 (1996) 2629-2634.
- F. Gerd-Uwe, R. Thomas, Electrochemical detection of DNA hybridization by means of osmium tetroxide complexes and protective oligonucleotides, Anal. Chem. 79 (2007) 2125-2130.
- Y.L. Zhang, Y. Wang, H.B. Wang, J.H. Jiang, G.L. Shen, R.Q. Yu, et al, Electrochemical DNA biosensor based on the proximity-dependent surface hybridization assay, Anal. Chem. 81 (2009) 1982-1987.
- R. Ren, C.C. Leng, S.S. Zhang, A chronocoulometric DNA sensor based on screenprinted electrode doped with ionic liquid and polyaniline nanotubes, Biosens. Bioelectron. 25 (2010) 2089-2094.

- [9] I. Sumio, Helical microtubules of graphitic carbon, Nature 354 (1991) 56-58.
 [10] N. Alexeyevaa, T. Laaksonenb, K. Kontturib, F. Mirkhalafc, D.J. Schiffrinc, K. Tammeveskia, Oxygen reduction on gold nanoparticle/multi-walled carbon nanotubes modified glassy carbon electrodes in acid solution. Electrochem. Commun. 8 (2006) 1475-1480.
- [11] H. Xu, K.C. Zheng, Y. Chen, Y.Z. Li, L.J. Lin, H. Li, et al, Effects of ligand planarity on the interaction of polypyridyl Ru(II) complexes with DNA, Dalton Trans. 3 (2003) 2260-2268.
- D.W. Pang, H.D. Abruňa, Interactions of benzyl viologen with surface-bound single- and double-stranded DNA, Anal. Chem. 72 (2002) 4700-4706.
- [13] E. Grueso, G. López-Pérez, M. Castellano, R. Prado-Gotor, Thermodynamic and structural study of phenanthroline derivative ruthenium complex/DNA interactions: Probing partial intercalation and binding properties, J. Inorg. Biochem. 106 (2012) 1-9.
- M. Ganeshpandian, R. Loganathan, S. Ramakrishnan, A. Riyasdeenb, M.A. Akbarshac, M. Palaniandavara, Interaction of mixed ligand copper(II) complexes with CT DNA and BSA: Effect of primary ligand hydrophobicity on DNA and protein binding and cleavage and anticancer activities, Polyhedron 52 (2013) 924-938.
- A. Terenzi, G. Barone, A. Silvestri, A.M. Giuliani, A. Ruggirello, V.T. Liveri, The interaction of native calf thymus DNA with Fe(III)-dipyrido[3,2-a:2',3'c]phenazine, J. Inorg. Biochem. 103 (2009) 1-9.
- G. Lan, R. Dong, N. Yu, L. Zhang, Y. Ma, C. Yang, et al, Construction of three new coordination polymers based on 5-ethyltetrazole (ET) generated via in situ cycloaddition reaction, Inorg. Chem. Commun. 24 (2012) 190-194.
- Y.M. Song, J.W. Kang, J.Z. Gao, Y.F. Feng, Study on the effect of cobalt (III) complexes with DNA, Chin. J. Inorg. Chem. 16 (2000) 53-57.
- Q.L. Zhang, J.H. Liu, P.X. Zhang, X.Z. Ren, C.H. Li, W.L. Hong, et al, Effects of ligands shape on DNA-binding of copper(II) polypyridyl complexes. Chin. J. Inorg. Chem. 21 (2005) 344-348.
- L.S. Li, Z.B. Huang, Y.X. Wang, X. Liu, Y.P. Li, X.H. Ge, Study on the Interaction of Water-Soluble p-(N, N-Dimethylaminomethyl) calix[8] arene with DNA by fluorescent spectrometry, Spectrosc. Spectr. Anal. 25 (2005) 1088-1091.
- M.T. Carter, M. Rodriguez, A.J. Bord, Voltammetric studies of the interaction of metal chelates with DNA. 2. Tris-chelated complexes of cobalt (III) and iron(II) with 1,10-phenanthroline and 2,2'-bipyridine, J. Am. Chem. Soc. 111 (1989) 8901-8911.